TẠP CHÍ KHOA HỌC
TRƯỜNG ĐẠI HỌC QUY NHƠN

Tổng hợp cấu trúc opal nghịch đảo Co_3O_4 có độ xốp cao ứng dụng làm vật liệu xúc tác điện hóa hiệu suất cao

Nguyễn Văn Nghĩa[1], Phan Thế Vinh[2], Nguyễn Thị Lệ Thanh[3], Nguyễn Thị Hồng Trang[1,*]

[1]Khoa Khoa học tự nhiên, Trường Đại học Quy Nhơn, Việt Nam
[2]Cao học ngành Vật lý chất rắn khóa 22, Khoa Khoa học tự nhiên, Trường Đại học Quy Nhơn, Việt Nam
[3]Cao học ngành Vật lý chất rắn khóa 20, Khoa Khoa học tự nhiên, Trường Đại học Quy Nhơn, Việt Nam

Ngày nhận bài: 27/09/2021; Ngày sửa bài: 02/12/2021;

Ngày nhận đăng: 02/12/2021; Ngày xuất bản: 28/02/2022

TÓM TẮT

Bằng phương pháp dùng khuôn là các quả cầu polystyrene, kết hợp với quá trình nhiệt phân trong không khí, chúng tôi đã chế tạo thành công vật liệu nano Co_3O_4 cấu trúc xốp có độ trật tự cao. Hình thái và cấu trúc tinh thể của vật liệu được khảo sát bằng phương pháp kính hiển vi điện tử quét (SEM) và phương pháp nhiễu xạ tia X (XRD). Kết quả ảnh SEM cho thấy khoảng cách giữa các lỗ xốp cỡ vài đến vài chục nano mét và đường kính trung bình của các lỗ xốp trong khoảng 260 – 300 nm. Kết quả phân tích phổ XRD của mẫu cho thấy vật liệu được tổng hợp có cấu trúc tinh thể dạng lập phương. Tính chất xúc tác điện hóa của vật liệu được khảo sát thông qua phản ứng tổng hợp oxi từ nước. Kết quả cho thấy hiệu suất vượt trội của cấu trúc xốp nano so với cấu trúc hạt nano.

**Tác giả liên hệ chính.*
Email: nguyenthihongtrang@qnu.edu.vn

https://doi.org/10.52111/qnjs.2022.16102

JOURNAL OF SCIENCE
QUY NHON UNIVERSITY

Facile synthesis of highly ordered mesoporous Co_3O_4 inverse opals as a high-performance electrocatalyst

Nguyen Van Nghia,[1] Phan The Vinh,[2]
Nguyen Thi Le Thanh,[3] Nguyen Thi Hong Trang[1,*]

[1]Faculty of Natural Sciences, Quy Nhon University, Vietnam
[2]22nd Master Class of Solid State Physics, Faculty of Natural Sciences, Quy Nhon University, Vietnam
[3]20st Master Class of Solid State Physics, Faculty of Natural Sciences, Quy Nhon University, Vietnam

Received: 27/09/2021; Revised: 02/12/2021;

Accepted: 02/12/2021; Published: 28/02/2022

ABSTRACT

In this study, highly ordered mesoporous Co_3O_4 inverse opals are synthesized using polystyrene beads as a hard template, followed by a calcination in air. The morphology and crystalline structure of the mesoporous Co_3O_4 are investigated by scanning electron microscopy and X–ray diffraction techniques. The characterizations reveal that the thickness of the pore walls of the inverse opals is in the range of a few to a few tens of nanometers, the average diameter of the pores is in the range of 260 – 300 nm, and the mesoporous Co_3O_4 has a spinel crystalline structure. The electrocatalytic properties of the materials are investigated by the oxygen evolution reaction. The results show a superior activity of the mesoporous structure with a small Tafel slope and a low overpotential in the alkaline medium compared to the nanoparticle counterpart.

1. INTRODUCTION

Renewable energy sources have been developed rapidly due to the world's growing energy demands and serious environmental threat caused by the depletion of natural fossil resources such as coal, oil, and natural gas. Even so, currently renewable energy sources only account for a very small part of the total global energy consumption. The renewable energy is still not popular in the world because the extraction technology is still limited, making product cost still high.

Catalytic splitting of water into hydrogen and oxygen provides a potential path to product clean H_2 and O_2 for human society as the input materials for fuel cells, and metal–air batteries such as lithium–air batteries, zinc–air batteries. However, one of major hurdles of water electrolysis is anodic oxygen evolution reaction (OER) which needs high onset potential and shows slow sluggish kinetics due to four-electron transfer process. Consequently, extensive efforts have been undertaken to develop highly efficient catalysts with low onset potential and promoted reaction kinetics. Many materials with different structures have been studied recently to improve OER efficiency.

Typically, ruthenium oxide (RuO_2) and iridium oxide (IrO_2) have been proven to be

*Corresponding author.
Email:nguyenthihongtrang@qnu.edu.vn

https://doi.org/10.52111/qnjs.2022.16102

highly efficient OER catalysts.[1] Unfortunately, these noble metal oxide catalysts suffer from poor chemical stability in alkaline media and high price, which limit their practical large-scale application as water splitting anodes. Therefore, design and development of OER catalysts with low cost and high activity has attracted considerable attention, and lots of efforts have been made.[2,3]

Cobalt oxide (Co_3O_4) has been intensely studied for electrochemical energy conversion and storage, including as an electrocatalyst for the water oxidation/OER, in lithium-ion batteries, and as supercapacitors, due to its excellent catalytic properties and high corrosion stability. The low cost and earth abundance of Co_3O_4 have suggested it to be a highly promising substitute for rare metal based catalysts.[2,3] Moreover, Co_3O_4 with different morphologies, such as hollow fluffy cage,[3] three-dimensional ordered nanoporous,[4] core-shell,[5] has been used as efficient OER catalyst. As the surface area and electronic states of Co_3O_4 are two of the main contributors for its catalytic performance, substantial work has been focused on developing new synthetic approaches to realize a variety. Additionally, mesoporous nanostructures are beneficial for promoting electrochemical performance of electrodes due to their interconnected pores, large specific surface area, controllable pore size and pore wall composition.[6,7] Template method has been considered as one of the most convenient and effective methods to prepare mesoporous inverse opal structures.

In this paper, Co_3O_4 with mesoporous inverse opal structure (Co_3O_4 IO) is fabricated on nickel foam (NF) substrates via chemical method with polystyrene (PS) beads as hard template, followed by the calcination process in air. The influence of fabrication conditions such as solution concentration, calcinated temperature on morphology and crystal structure are studied by SEM and XRD analytic techniques. The electrocatalytic properties for OER of as-synthesized materials are also studied.

2. EXPERIMENTAL

2.1. Nickel foam substrate preparation

Nickel foam susbtrate with an area of 1.0 cm x 1.0 cm was ultrasonically cleaned for 5 minutes in a 0.5 m hydrochloric acid (HCl) and for 30 minutes in ethanol (EtOH) and distilled (DI) water to remove any contaminants and amorphous surface oxides, and was dried in box furnace at 60 ^oC for 12 h in air.

2.2. Synthesis of PS nanobeads

PS spheres were prepared by emulsion polymerization using sodium dodecyl Sulfafe (SDS, Sigma Aldrich), sotassium persulfafe (PPS, Sigma Aldrich), and aqueous distilled water as emulsifier, initiator, and dispersion medium, respectively. A mixture of 8 mg SDS surfactants, 100 mg PPS initiators and 30 ml deionized water was kept to 70 °C for 30 minutes under N_2 flow in a three-necked reaction flask. 6 ml of styrene monomers, which had been filtered with alumina, was quickly injected to the solution. After polymerization at 70 °C for 4 h, the obtained PS dispersion was dialysated filtered in deionized water for 3 days to remove unreacted reagents. PS beads of 280 nm average diameter were obtained.

2.3. Co_3O_4 IO fabrication

The substrates (NF or glass subtrates) as electrodes were vertically immersed into 50 mL of PS solution which was prepared by diluting 1 ml as-prepared PS bead solution with 35 ml of distilled water and 14 ml of anhydrous ethanol. By keeping the sustrates in the PS solution at 65 °C for 48 h until the solution was completely evaporated, PS beads were uniformly coated on the electrodes. As a cobalt oxide source, cobalt nitrate hexahydrate ($Co(NO_3)_2.6H_2O$, Sigma Aldrich) was slowly added into anhydrous ethanol, and stirred at ambient condition for 1 h. After stirring, $Co(NO_3)_2.6H_2O$ solution was dropped on PS coated substrate (20 µl cm^{-2}) by micropipette. The electrodes were dried overnight in ambient conditions, followed by thermal annealing at 90 °C for 1 h in air. Finally,

https://doi.org/10.52111/qnjs.2022.16102

these $Co(NO_3)_2.6H_2O$-treated PS/substrates were transferred to box furnace, and annealed at 450 °C for 2 h (ramping rate of 5 °C min^{-1}) in air to form Co_3O_4 IO with a removal of PS template. The synthesized process of Co_3O_4 IO is summarized in Figure 1.

In this paper, we studied different samples by varying the synthetic parameters with $Co(NO_3)_2.6H_2O$ concentration of 0.1 M; 0.2 M and 0.4 M and calcinated temperatures of 300 ºC, 450 ºC and 600 ºC. The samples with different fabricated conditions denoted as M01.450, M02.450, M04.450, M02.300, and M02.600 respectively.

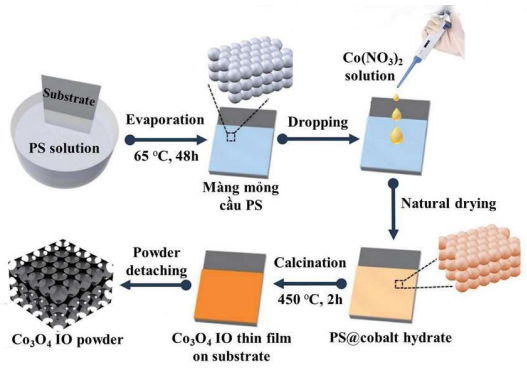

Figure 1. The fabrication process of Co_3O_4 IO

2.4. Characterization and investigation of electrochemical properties of Co_3O_4 IO electrode

Scanning electron microscopic (SEM) measurement was performed using a HITACHI S–4800 microscope to observe the morphology of Co_3O_4 IO samples. The crystal structure of as-synthesized materials was characterized by using X-ray diffraction (D8 Advance Bruker). The crystallinity and chemical structure of the Co_3O_4 IO were studied by a Raman spectroscopy (XploRA–Horiba).

To evaluate the electrochemical performance of the electrodes, experiments were carried out in a three-electrode electrochemical cell using potentiostat (DY2300). The as-prepared Co_3O_4 IO on substrate were used as working electrode, electrode, Platinum (Pt) wire and Ag/AgCl (saturated in KCl) were used as the counter and reference electrode. The electrolyte was 1.0 M KOH. For OER performamce, LSV polarization curves were recorded from 0.2 - 0.8 V versus saturated Ag/AgCl at a scan rate of 10 mV s^{-1} under N_2 medium.

3. RESULTS AND DISCUSSION

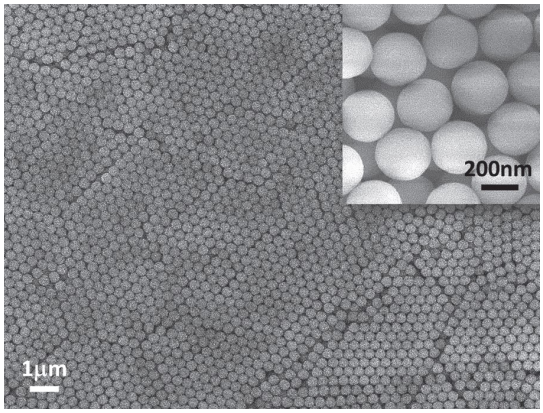

Figure 2. SEM image of PS beads deposited on glass substrate (the inset is the enlarged image of corresponding sample).

The SEM image was represented to investigate the morphology of the nanostructures involved in each step of the entire fabrication process in Figure 1. Figure 2 shows the SEM image of PS beads deposited on the glass substrate, evidencing the relatively uniform diameter, smooth surface, and well-ordered arrangement. The average diameter of the PS beads is about 270 nm.

SEM images of Co_3O_4 IO at different prepared conditions with $Co(NO_3)_2.6H_2O$ concentrations of 0.1 M; 0.2 M; 0.4 M (at the calcination temperature of 450 ºC) are shown in Figure 3.

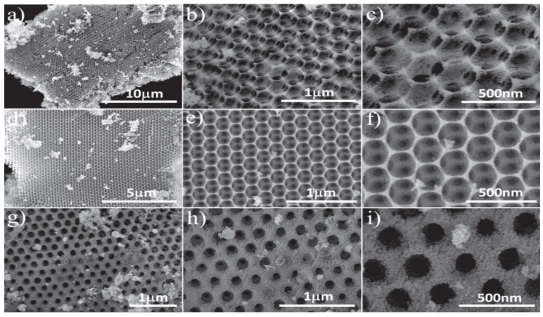

Figure 3. SEM images of Co_3O_4 IO with concentrations of $Co(NO_3)_2.6H_2O$: 0.1 M (a, b, c); 0.2 M (d, e, f); 0.4 M (g, h, i).

https://doi.org/10.52111/qnjs.2022.16102

At concentration of 0.1 M, the wall between the pores of IO structure is thin, the average diameter of the pore is approximately 300 nm (Fig. 3 a, b, c). With this morphology, the electrode has a large surface area, high porosity, but weak inter-pore adhesion leading to a fragile structure. When increasing the concentration to 0.2 M, the obtained Co_3O_4 IO structure has a fairly homogeneous and clear shape, with the honeycomb-like morphology. The thickness between the pores increases, the diameter of the pores decreases with the average value of about 270 nm (Fig. 3d, e, f). Although the surface area of material in this condition is slightly reduced, the morphology is more uniform.

Continuing to increase the concentration to 0.4 M, the thickness between the pores increased, so the surface area dramatically decreased, and the material morphology was not uniform anymore. The diameter of the pores is now greatly reduced, averaging only 170 nm (Fig. 3g, h, i). From the SEM images, it can be seen that changing the concentration of $Co(NO_3)_2.6H_2O$ has affected the morphology as well as the texture of the Co_3O_4 IO material. Based on the above analysis results, we found that 0.2 M is the optimal condition for material synthesis and research.

Calcination temperature is also an important parameter that can affect the morphology of the material. Figure 4 shows the SEM image of the Co_3O_4 IO material calcined at 600 ºC (at $Co(NO_3)_2.6H_2O$ concentration of 0.2 M). In comparison with the samples synthesized at the calcination temperature of 450 ºC (Fig. 3d, e, f), the thickness of the wall between the pores is thinner, so the structure of material easily gets colaped. We predict that if the temperature continues to increase, it is very likely that this structure will not be maintained, and the honeycomb shape will be broken. If the sample is calcinated at a temperature lower than 450 ºC, this temperature is not high enough to completely ignite the PS[8] to form a porous nanostructure. Combined with the above analysis results, the limit calcination temperature for the IO sample can be selected as 600 ºC or less, and the optimal temperature of 450 ºC was chosen in this study.

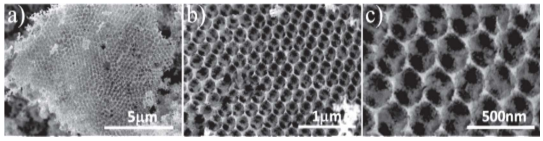

Figure 4. The SEM image of the Co_3O_4 IO material calcined at 600 ºC at different magnifications.

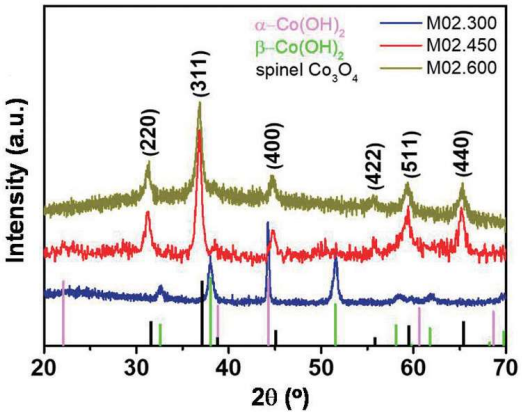

Figure 5. The XRD patterns of the Co_3O_4 IO samples at $Co(NO_3)_2.6H_2O$ concentration of 0.2 M and calcination temperature of 300 ºC, 450 ºC and 600 ºC, respectively.

The XRD patterns of the Co_3O_4 IO structures at $Co(NO_3)_2.6H_2O$ concentration of 0.2 M and calcination temperature of 300 ºC, 450 ºC and 600 ºC are shown in Figure 5. XRD results reveal that, at the 300 ºC, the material only exists phase α, β of $Co(OH)_2$ (JCPDS No. 30-443). At the 450 ºC and 600 ºC, XRD patterns exhibit diffraction peaks at 31.2º, 36.8º, 44.6º, 55.5º, 59.3º and 65.2º, which are assigned to (220), (311), (400), (422), (511) and (440) faces of cubic crystallite Co_3O_4 (JCPDS No.42–1467). No peaks ascribed to other impurities can be found, revealing the high purity of as-synthesized spinel oxides. This result indicates that cobalt precursor has been completely transformed into crystalline Co_3O_4 at the temperature higher 450 ºC.

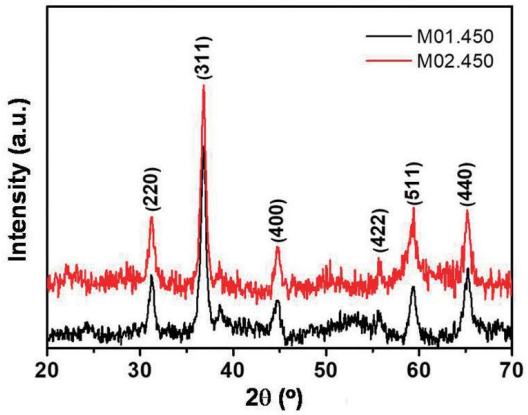

Figure 6. The XRD patterns of Co_3O_4 IO at calcination temperature of 450 °C and $Co(NO_3)_2.6H_2O$ concentrations of 0.1 M and 0.2 M.

Figure 6 shows the XRD profiles of samples synthesized at $Co(NO_3)_2.6H_2O$ concentration of 0.1 M and 0.2 M and calcination temperature of 450 ºC (M01.450 and M02.450). The XRD patterns of two samples at different concentrations has exactly the same peak positions and are confirmed to agree with reported spinel cobalt oxide. This result indicates that $Co(NO_3)_2.6H_2O$ concentration does not affect the crystal structure of the as-synthesized material.

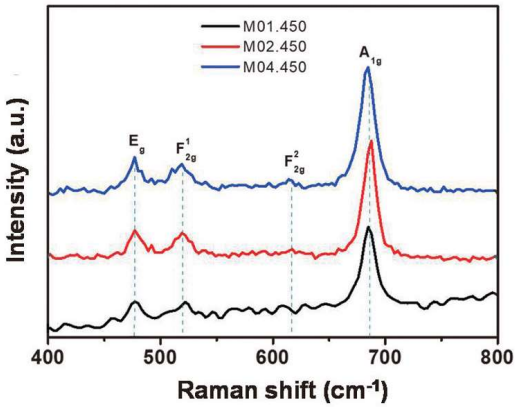

Figure 7. Raman spectra of samples synthesized at different $Co(NO_3)_2.6H_2O$ concentrations and calcination temperature of 450 °C (M01.450, M02.450, and M04.450).

Raman spectra of samples samples synthesized at different $Co(NO_3)_2.6H_2O$ concentrations and calcination temperature of 450 °C (M01.450, M02.450, and M04.450) are presented in Figure 7. As revealed by these results, there are four Raman-active modes at 482, 521, 618, and 690 cm^{-1} attributed to the E_g, F^1_{2g}, F^2_{2g}, and A^1_g vibration modes of the cubic structure of Co_3O_4,[9] further confirms the formation of Co_3O_4 spinel, which is corroborated by the XRD. From the XRD and raman results, it is clearly revealing that cobalt salt concentration affects only the morphology (SEM results) without changing the crystal structure of Co_3O_4 IO.

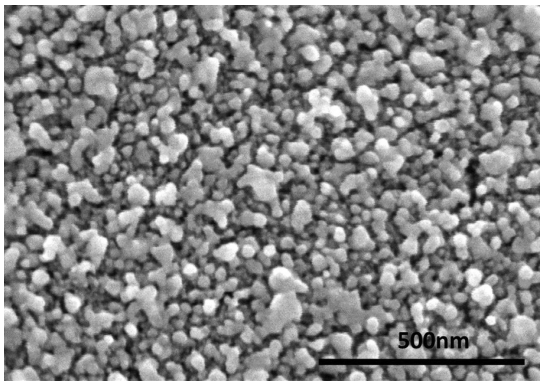

Figure 8. SEM image of the Co_3O_4 nanoparticle was synthesized by hydrothermal method.

To evaluate the electrochemical property of Co_3O_4 IO, we also synthesized Co_3O_4 nanoparticle materials (denoted as Co_3O_4 NP) as the reference by hydrothermal method at 120 ºC, 12 h. The cobalt precursor is also a cobalt nitrate salt, but without the PS template. The morphology of the Co_3O_4 nanoparticles is shown in Figure 8.

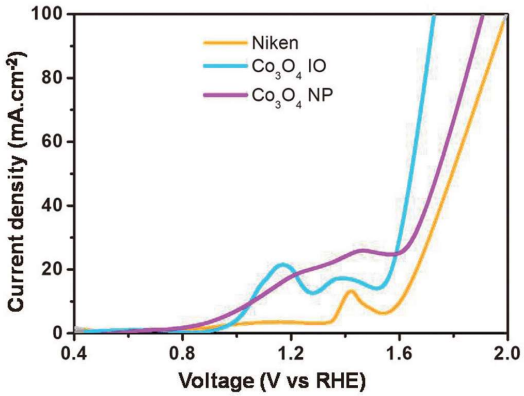

Figure 9. LSV characteristics of Co_3O_4 IO (sample M02.450) and Co_3O_4 NP as the reference.

https://doi.org/10.52111/qnjs.2022.16102

Figure 9 compares LSV characteristics of Co_3O_4 IO and Co_3O_4 NP materials fabricated on NF substrates. The graphs show that the overpotential values (η) of the NF substrate, Co_3O_4 IO, and Co_3O_4 NP (at the current density of 30 $mA.cm^{-2}$) is 1.71 (V), 1.65 (V), and 1.60 (V), respectively. Thus, compared with the Co_3O_4 NP, the Co_3O_4 IO material needs a much lower overpotential value. Moreover, the LSV characteristic curve of the Co_3O_4 IO shows higher slope, demonstrating the OER reaction rate of the Co_3O_4 IO sample is much faster than that of than that of Co_3O_4 NP counterpart. The above results confirm the outstanding catalytic performance of the Co_3O_4 IO sample.

This result can be explained as follows: The NF substrate has a three-dimensional (3D) porous structure with high surface area, whereas the distribution of the catalyst on the entire substrate is uniform, which greatly increases the catalytic active sites of the material. Meanwhile, the regular empty spaces, surrounded by the mesoporous walls composes of tiny nanoparticles (size 5 - 7 nm), are interconnected by the pores/voids where the removed PS spheres have resided in contact with each other. The interconnected voids can act as diffusion channels, and hence, facilitating the charge exchange process, increasing the conductivity of the Co_3O_4 IO catalyst. Thus, the high catalytic performance of Co_3O_4 IO is demonstrated to be mainly attributed to both high surface area and good electrical conductivity. These results seem to hint at the interest in Co_3O_4 IO as an electrochemical catalyst for the OER process.

4. CONCLUSION

The Co_3O_4 ordered porous architecture, so-called inverse-opal structure has been successfully fabricated by chemical method using PS spheres as hard template, followed by calcination process in air. The morphology of the IO structute changes in terms of pore diameter and wall thickness of interconnected voids with the concentration of $Co(NO_3)_2.6H_2O$ and the calcination temperature. XRD patterns confirm the as-prepared IO material has a cubic crystal structure of Co_3O_4. We believe this work represents a valuable addition focusing on the importance of the IO structure to improve the electrocatalytic performance of Co_3O_4-based electrodes in OER. This contribution is therefore expected to further encourage studies of electrode design in electrochemical water-splitting, and metal-air batteries such as lithium-air batteries, and zinc-air batteries.

Acknowlegment

This work is funded by the Vietnam Ministry of Education and Training, under grant number B2020-DQN-06.

REFRENCES

1. E. G. L. Michael, F. Stephane. Mechanism of oxygen reactions at porous oxideelectrodes. Part 2—Oxygen evolution at RuO_2, IrO_2 and $Ir_xRu_{1-x}O_2$ electrodes in aqueous acid and alkaline solution, *Physical Chemistry Chemical Physics,* **2011**, *13*, 5314-5335.
2. M. Bajdich, M. Garcia-Mota, A. Vojvodic, J. K. Norskov, A. T. Bell. Theoretical investigation of the activity of cobalt oxides for the electrochemical oxidation of water, *Journal of the American Chemical Society*, **2013**, *135*, 13521–13530.
3. J. Rosen, G. S. Hutchings, F. Jiao. Ordered mesoporous cobalt oxide as highly efficient oxygen evolution catalyst, *Journal of the American Chemical Society*, **2013,** *135,* 4516–4521.
4. W. Y. Xia, N. Li, Q. Y. Li, K. H. Ye, C. W. Xu. Au-$NiCo_2O_4$ supported on threedimensional hierarchical porous graphene-like material for highly effective oxygen evolution reaction, *Scientific Reports*, **2016,** *6*.
5. Z. Zhuang, W. Sheng, Y. Yan. Synthesis of monodispere Au@Co_3O_4 core-shell nanocrystals and their enhanced catalytic activity for oxygen evolution reaction, *Advanced Materials*, **2014,** *26*, 3950 - 3955.

6. X. Zou, J. Su, R. Silva, A. Goswami, B. R Sathe, T. Asefa. Efficient oxygen evolution reaction catalyzed by low-density Ni-doped Co_3O_4 nanomaterials derived from metalembedded graphitic C_3N_4, *Chemical Communications*, **2013**, *49*, 7522 - 7524.

7. Seol A Cho, Yu Jin Jang, Hee-Dae Lim, Ji-Eun Lee, Yoon Hee Jang, Trang Thi Hong Nguyen, Filipe Marques Mota, David Fenning, Kisuk Kang, Yang Shao-Horn, Dong Ha Kim. Hierarchical Porous Carbonized Co_3O_4 Inverse Opals via Combined Block Copolymer and Colloid Templating as Multifunctional Electrocatalysts and Cathodes in LiO_2 Battery, *Advanced Energy Materials,* **2017***, 7*.

8. C. Konstantinos, E. EleniPavlidou, D. B. Vouvoudi. Decomposition kinetic and mechanism of syndiotactic polystyrene nanocomposites with MWCNTs and nanodiamonds studied by TGA and Py-GC/MS, *Thermochimica Acta*, **2014,** *583*, 15-24.

9. F. Gu, C. Li, Y. Hu, L. Zang. Synthesis and optical characterization of Co_3O_4 nanocrystals, *Journal of Crystal Growth*, **2007**, *304,* 369-373.

https://doi.org/10.52111/qnjs.2022.16102